
Aerodynamic Evaluation of Different Car Carrier Devices for Drag Reduction Using CFD

Daniel Acevedo-Giraldo¹, Laura Botero-Bolívar¹, Daniel Munera-Palacio², Juan Guillermo García-Navarro²

How to cite

Acevedo-Giraldo D  <https://orcid.org/0000-0002-1861-2393>

Botero-Bolívar L  <https://orcid.org/0000-0002-9824-1173>

Munera-Palacio D  <https://orcid.org/0000-0002-7010-2438>

García-Navarro JG  <https://orcid.org/0000-0002-8540-3196>

Giraldo DA; Botero L; Palacio DM; Navarro JGG (2018) Aerodynamic Evaluation of Different Car Carrier Devices for Drag Reduction Using CFD. J Aerosp Technol Manag, 10:e4018. doi: 10.5028/jatm.v10.971.

ABSTRACT: Aerodynamic of commercial trucks has been extensively studied due to their impact on fuel efficiency; reducing consumption is one of the most important and challenging issues for the trucking industry. In this paper, several Computational Fluid Dynamic (CFD) simulations are performed to evaluate the drag of a standard car carrier and its different modifications. Therefore, several covers, which act as aerodynamic devices, are tested to determine their effectiveness in fuel consumption. The study compares the drag coefficients, velocity vectors, pressure contours, and turbulence kinetic energy of different fairing configurations. The results show that, although all covers reduce the drag coefficient compared to the conventional car carrier, two of them have significant drag reductions.

KEYWORDS: Aerodynamics, Car carrier, Computational fluid dynamics, Drag coefficient, Fuel consumption.

INTRODUCTION

The study of aerodynamic drag, fuel consumption and gas emissions from heavy trucks are very important in the automotive industry. During the 1970s and 1980s, substantial efforts were expended to improve truck aerodynamics to reduce fuel consumption (Cooper 2003). Since these years, different players involved in road freight transport industry have understood that fuel consumption is one of the main factors that increases operating costs. Therefore, the use of aerodynamic improvements to reduce wind resistance in vehicles is one of the most important ways to tackle this problem (Schoon 2007; Roy and Srinivasan 2000). However, heavy commercial vehicles still have the lowest aerodynamic performance compared to other ground vehicles (Chowdhuru *et al.* 2013), mainly because their body shape and large frontal areas generate highly turbulent fluid flows with great pressure gradients. It is estimated that a 40-tonne articulated truck at 60 mph can consume four times more fuel than an average car (Mohamed-Kassim and Filippone 2010).

Fuel consumption caused by aerodynamic drag on heavy vehicles can vary widely because it is affected by different factors such as truck type, terrain topography, and road conditions. Mohamed-Kassim and Filippone (2010) calculated the fuel consumption

¹.Universidade de São Paulo – Escola de Engenharia de São Carlos – Departamento de Engenharia Aeronáutica – São Carlos/SP – Brazil. ².Universidad Pontificia Bolivariana – Aerospace Engineering Research Group – Medellín/Antioquia – Colombia.

Correspondence author: Juan Guillermo García Navarro | Universidad Pontificia Bolivariana – Aerospace Engineering Research Group | Circular 1 70-01 | 050031 – Medellín/Antioquia – Colombia | E-mail: juan.garcia@upb.edu.co

Received: Oct. 11, 2017 | Accepted: Feb. 11, 2018

Section Editor: T. John Tharakan



of a 40-tonne truck using two approaches, the Long-Haul Driving Cycle (LHDC) and the modified New European Driving Cycle (NEDC). Using the LHDC they estimated that 38.2% of fuel consumption is due to aerodynamic drag, while for the NEDC only 14.7% of the consumption is due to the drag. This difference is because the LHDC fits better when a truck runs a long-haul route, while the NEDC is more like driving in urban areas, where truck acceleration is the main fuel consumption. In another study, Holmberg *et al.* (2014) analyzed all the energy losses form for four types of heavy vehicles (trucks and buses) at different speeds. They found that at low speeds (20 km/h) aerodynamic drag only represents 2% of fuel consumption, while at high speeds (80 km/h) consumption can reach up to 20% of total fuel energy.

The fuel consumption is an important issue in road transport industry; the Center for Transportation Analysis calculated that medium and heavy trucks consumed 6012 trillion BTU in the US during 2014, which was the 23% of Domestic Transportation Energy (DTE) (Davis *et al.* 2016), being the second largest consumers after the light vehicles category (Fig. 1). If the average of drag losses of heavy vehicles were 20%, the drag losses would represent 4.6% of the DTE, which would be equivalent to 1204 trillion BTU. This means that any improvement in aerodynamic will represent an important fuel saving.

Car carrier vehicles are specialized commercial trucks designed to transport several cars efficiently, easily and safely. The type of car carriers used around the world varies by region and different configurations can be used according to country-specific regulations, however, most commercial car carriers can transport between five and nine cars, depending on the car size and the trailer model (NTG 2007; FHWA 2004). Their loading capacity changes depending on their specific application, e.g. there are fully covered car carrier vehicles that reduce their cargo capacity but ensure full protection of the transported cars, and there are vehicles with a very high trailer capacity with lower operating costs. There are also mixed trailers that can be used to transport a standard container when there are no cars to transport.

Like a standard truck, these vehicles are made up of three primary sections: the tractor section, where the engine and the cab are located; the trailer section where the payload is transported; and the wheel assembly section. It is estimated that the tractor generates 45% of the total drag and the trailer 30% (Hyams *et al.* 2011). In car carriers, the drag contribution of the trailer section is greater than any other type of truck due to their non-aerodynamic design, which causes the air moving through the metallic structure of the trailer and the cars transported.

The more accessories used to reduce drag, the lower the engine power required. McCallen *et al.* (2004) reported that drag force is more relevant at higher speeds, therefore, aerodynamic accessories are more effective as the vehicle speed increases. In general, the drag can be divided into pressure drag and friction drag. The former depends on the frontal area and the object shape, while the latter is produced by the viscosity interaction between a fluid flow and an object surface. On heavy ground vehicles, the pressure drag is the most dominant force, contributing more than 90% of the total drag produced (Wood 2004).

This paper studies the aerodynamics of a standard car carrier. The car carrier has a maximum capacity of seven cars. This research focuses on the effect of using different aerodynamic covers for tractor and trailer, which have the added benefits of protection against environmental factors, decreasing damage risk of the cargo transported, and reducing the total operational cost.

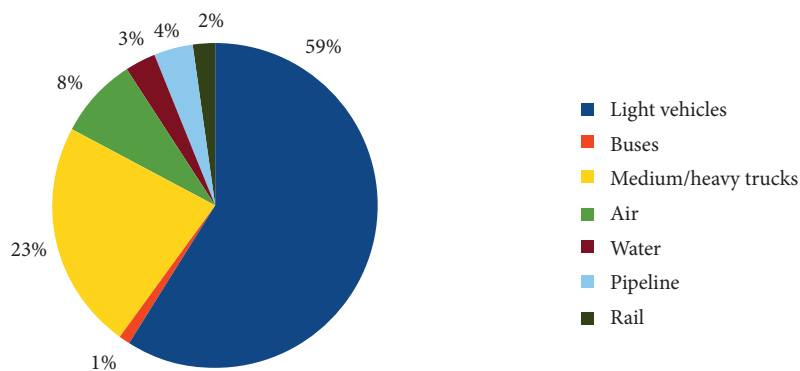


Figure 1. Percentages of domestic consumption of transportation energy in the US during 2014 (Davis *et al.* 2016).

The document is organized as follows. The first section presents the state of the art with the emphasis on CFD studies and experimental testing. The second section includes the numerical simulation approach that contains the geometry of the car carrier and its modifications, and also the definition of numerical simulation, i.e., computational domain, mesh, boundary conditions and mathematical model. The following section shows the numerical results and a brief fuel consumption estimation of each configuration. Finally, the conclusions and future works are discussed.

STATE OF THE ART: CFD AND EXPERIMENTAL SOLUTIONS

Truck manufacturers and freight carrier companies have redesigned and modified their trucks to improve the aerodynamic performance. Therefore, many studies have been conducted to reduce the aerodynamic drag in heavy vehicles. In most of the studies related to heavy trucks, aerodynamic developments are focused on the cab truck roof, the tractor-trailer gap, the rear trailer and the wheels (Cooper 2003).

Chowdhury *et al.* (2013) tested the drag of a 1/10 th scale semi-trailer truck model in a wind tunnel at various speeds and yaw angles using different combinations of fairings. They used fairings that cover the roof of the tractor, the tractor-trailer gap, and the wheel assembly zone. They found that any improvement in the front area of the truck has the most significant effect on drag. They obtained a 26% drag reduction for the best combination. They calculated that the cab roof fairing alone can reduce about 17% of drag, and if joined with the fairing for the tractor-trailer gap, the drag reduction can be up to 25.5%. A similar experimental study (Ortega *et al.* 2007) was conducted for three full-scale vehicle configurations in the NASA Ames 80×120 wind tunnel. In this study, different aerodynamic covers were evaluated, including tractor-trailer gap devices, trailer skirts, and trailer boat-tails; it was estimated that the best match of aerodynamic devices can achieve a fuel saving up to $15000 \text{ L}/2.012 \times 10^8 \text{ m}$ on a highway.

In another study (Mosaddeghi and Oveisi 2015), a CFD analysis was performed to evaluate the drag effect of supplementary parts on a semi-trailer truck. They used a combination of fairings, vanes, and flaps in different parts of the truck body achieving a 41% drag reduction. They also concluded that cab roof fairing is the device that most reduces the drag, representing 21% of total reduction. It is worth mentioning that in this study the angle position of the supplementary parts is deeply analyzed to obtain the angle values where the drag is smaller.

Other studies have focused on reducing drag force due to underbody flow in heavy vehicles. Rolling tires assembly account for 25% of the total aerodynamic drag in a passenger car (Wickern *et al.* 1997), while for a truck the rolling tires can be responsible for the 30% of the drag (Wood and Bauer 2003). It is also proved that drag is significantly affected by the ground clearance of the truck tractor and the trailer. In a study made by Hwang *et al.* (2016), panels curtaining the underspace between the front and the rear wheels of a truck trailer were proposed, in order to mitigate the drag caused by underbody flow. They evaluated different configurations of side skirts by wind tunnel tests and CFD, achieving a 5% total drag reduction. There are also many other modifications proposed by several authors aiming to reduce the drag in heavy vehicles; the review made by Choi *et al.* (2013) is a complete compendium of different proposals that includes forebody, base and underbody drag reduction devices. However, to the knowledge of the authors, there are no studies about aerodynamic of car carrier vehicles.

This project is mainly focused on aerodynamic simulations of different cover designs, therefore the selection of the cover materials, cost of implementation and regulatory issues are not discussed in this paper.

NUMERICAL SIMULATION APPROACH

Numerical simulations were computed in order to obtain and compare the drag produced for each configuration. The purpose of the aerodynamic analysis is to compare the total drag produced by the basic car carrier and each of its modified versions.

The different configurations of the car carrier are discussed below, as well as the computational domain, grid characteristics, boundary conditions and turbulence model.

GEOMETRY OF THE CAR CARRIER

Only this type of car carrier is evaluated because is the configuration most used in countries like Colombia (South America), where the state of roads and the topography restrict the use of bigger trailers. In Colombia, it is estimated that approximately 48% of roads are in flat terrain, 29% in undulating terrain and 23% in mountainous terrain (Pabon *et al.* 2011).

The car carrier and its respective covers were created by CAD software. The overall dimensions for the car carrier are shown in Table 1. Lateral and front view of the car carrier is shown in Fig. 2.

Table 1. Overall dimensions.

Geometrical Parameter	Quantity (m)
Overall Length	18.0
Overall Width	2.8
Overall Height	4.0
Trailer Length	13.0
Trailer Width	2.8
Trailer Height	3.5

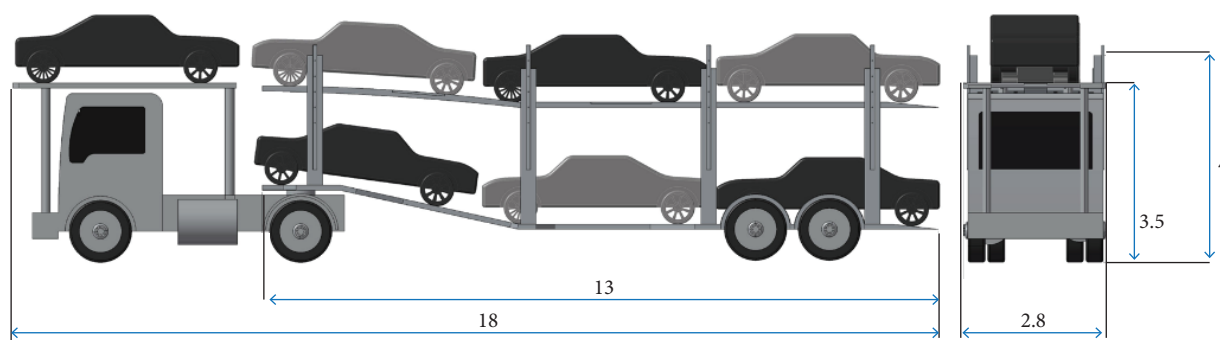


Figure 2. Overall dimensions (m).

AERODYNAMIC SOLUTIONS

The aerodynamic improvements tested are basically covers that aim to reduce the turbulence and flow recirculation generated around the cars transported. Figure 3 shows all the configurations used to simulate and compare the forces acting on them. The baseline configuration (C0) has no covers or modifications (Fig. 3a). Configuration 1 (C1) (Fig. 3b) has an aerodynamic cover over the tractor protecting the car transported located most upstream, deflecting the flow, and delaying the wake formation downstream. Lateral covers in configuration 2 (C2) (Fig. 3c) try to prevent crosswind in the trailer. Configuration 3 (C3) (Fig. 3d) uses the cover of C1 and a full cover of the trailer section in order to reduce the air stagnation between the carried cars. For these fourth configurations, as will be discussed below, C0 reported the highest drag while C3 the lowest. However, C3 will have a higher implementation and operational costs due to the cover price and the added weight related to the fuel consumption. Therefore, C1 is an intermediate proposal with lower drag than C0 and lower weight and price than C3.

The two additional configurations are similar to C1 with flow deflectors. Configuration 4 (C4) (Fig. 3e) adds a deflector at the upper end of the cover, and configuration 5 (C5) (Fig. 3f) has deflectors at the upper end and the sides of the cover. These flow deflectors are proposed for a greater delay of a fully turbulent flow.

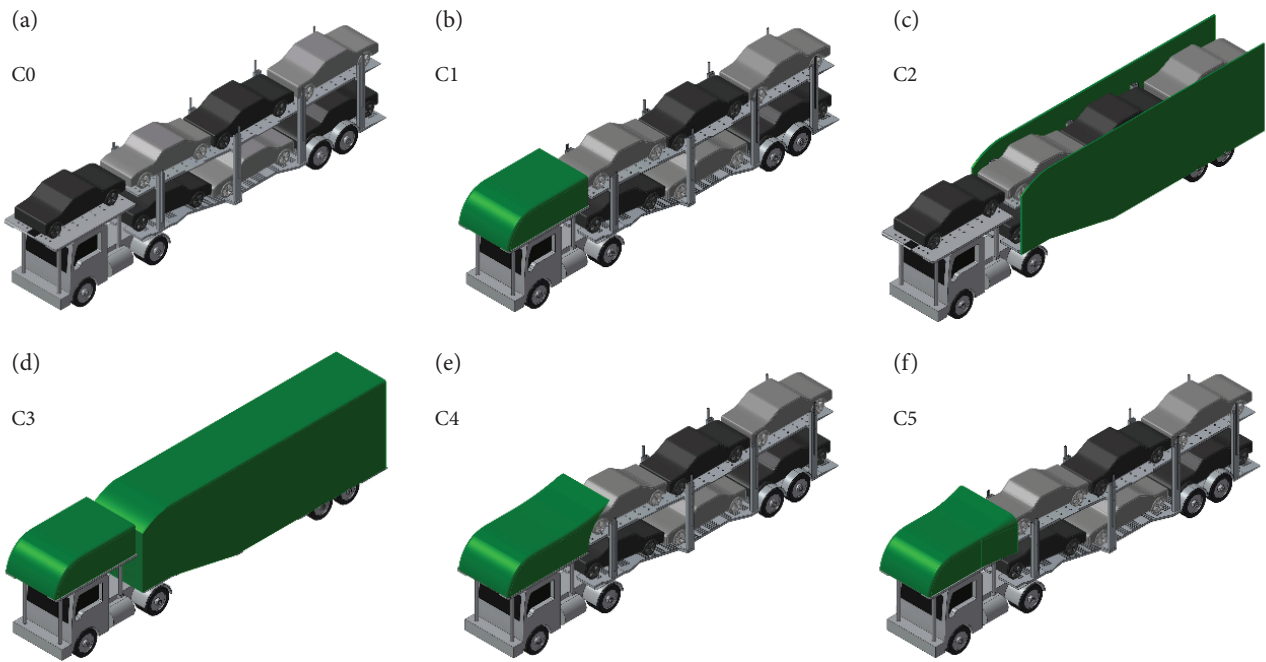


Figure 3. Initial and modified car carrier models.

COMPUTATIONAL DOMAIN

The size of the computational domain was defined to simulate a continuous medium or unbounded flow field. Hence, the size of the computational domain was created by ensuring the flow over the truck is not affected by the boundaries of the fluid domain. The size of the fluid domain was defined based on the Length (L), Width (W), and High (H) of the car carrier, where the dimensions of the computational domain are $5 W \times 4 H \times 11 L$, which are equivalent to $20 \text{ m} \times 7.2 \text{ m} \times 220 \text{ m}$. Figure 4 shows the lateral and front views of the domain. The length from the rear of the trailer to the outlet was defined by a convergence study. We varied this length between $2 L$ and $12 L$ and calculated the drag coefficient keeping the same refinement parameters in each case. As is shown in Fig. 5, results indicated that the drag coefficient converges to a total length of $11 L = 2 L + L + 8 L$.

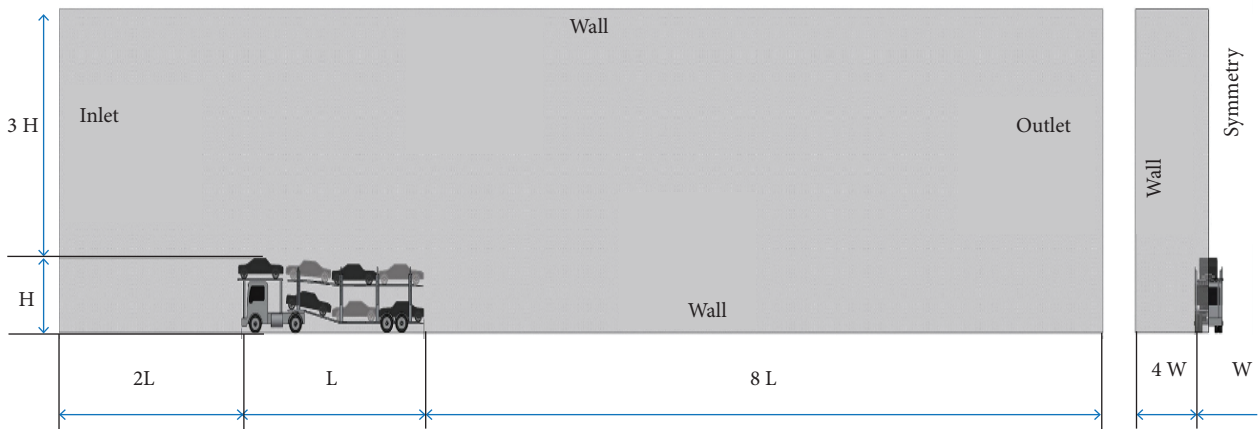


Figure 4. Domain dimensions.

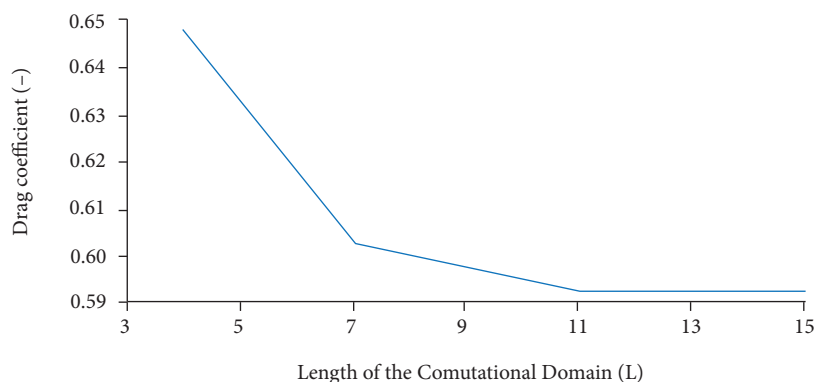


Figure 5. Total Length Convergence.

GRID STRATEGY

An unstructured mesh with tetrahedral elements were used in all computational domains, refined in almost all surfaces of the truck (tractor, wheels, cars transported, and some structural elements) and in regions where the flow has high gradients, such as downstream from the trailer, in order to capture and include all the flow behavior around the body. Coarser grids were used far from the truck where the flow is almost uniform in order to reduce computational time. Moreover, a grid independence study was carried out in order to guarantee the element size does not affect the results. Figure 6 shows the variation of the drag coefficient as a function of the number of elements, where six different meshes were evaluated. The mesh independence study showed that the drag force converges at approximately 14 millions of elements and 3 millions of nodes. The relative error of the drag coefficient of the mesh chosen with respect to the thinnest mesh (22 million elements) is less than 0.5%.

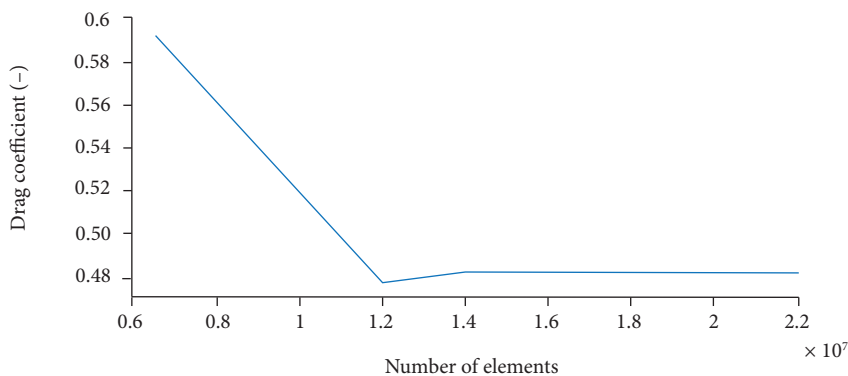


Figure 6. Mesh Independence.

Some mesh metrics controls were analyzed to determine mesh convergence: skewness, element quality, and aspect ratio. These parameters were in the correct range according to (Versteeg and Malalasekera 2007). We also guaranteed a wall function (log law) for the elements of the boundary layer of the truck surface with values between 30 and 500.

BOUNDARY CONDITIONS

All vehicles were simulated at 60 km/h, which is the average velocity of a truck that moves in a country like Colombia where only the 73% of roads are paved, from these paved roads 49% have good conditions, 28% regular conditions, and 23% poor conditions (Pabon *et al.* 2011). For boundary conditions, the symmetry of the truck was used to simulate only half the fluid

domain and reduce the computational cost, the roof of the domain was defined as a wall with slip condition, the floor as a moving wall, and all the truck parts, including wheels, as a wall with non slip condition. The reference values are in Table 2, and a detailed description of the boundary conditions is shown in Table 3. Additionally, for turbulence parameters, the inlet and outlet have a turbulent intensity of 5% and a turbulent viscosity ration equal to 10; for the walls with no slip shear conditions the roughness height is 0 m and the roughness constant is 0.

Table 2. Reference values.

Property	Value	Unit
Viscosity	1.7894×10^{-5}	Pa × s
Density	1.225	Kg/m ³
Reference Area	13.3	m ²
Pressure	101325	Pa

Table 3. Boundary conditions.

Boundary condition name	Boundary condition type	Value	Unit
Inlet	Velocity inlet	16.7	m/s
Wall (Car Carrier)	Wall with no slip shear condition	0	m/s
Wall (Wheels)	Wall with no slip shear condition and without rotation	0	m/s
Wall (Road)	Wall with no slip shear condition	16.7	m/s
Wall (Roof and Side)	Wall with slip shear condition	0	Pa
Symmetry	Symmetry	-	-
Outlet	Pressure outlet	0	Pa

MATHEMATICAL MODEL

The numerical simulations were evaluated using the commercial software Ansys - FLUENT, a widely accepted computational tool which works with the finite volume method. For more details on this CFD code see (ANSYS 2009).

In this problem, the fluid flow is assumed in a steady state, incompressible, and fully turbulent. For this case, is solved the Navier-Stokes (NS) equation where the unknowns are the velocity \mathbf{u} and the pressure p . The incompressible condition is forced by the continuity equation .

Since the NS equation alone cannot predict fluid flows at high Reynolds numbers, it was necessary to include a turbulence model to the system of equations. To maintain simplicity, we used the Realizable $\kappa - \epsilon$ model, which adds the transport equations of turbulent kinetic energy κ and turbulent dissipation ϵ (Shih *et al.* 1995). These equations, among others, are a function of the eddy viscosity $\mu_t = \rho C_\mu \kappa^2 / \epsilon$, where C_μ depends on the strain tensor, the rate-of-rotation tensor, and the angular velocity. For the standard $\kappa - \epsilon$, C_μ is a constant.

The Realizable $\kappa - \epsilon$ turbulence model have shown better results than the standard $\kappa - \epsilon$ model for fluid flows that includes recirculation, boundary layers under strong adverse pressure gradients, and flow separation (Mohamed *et al.* 2015).

The Realizable $\kappa - \epsilon$ model was compared against the SST $\kappa - \omega$ model (Menter 1994) to evaluate the difference between the results. The simulations showed a variation of less than 1% on the drag coefficient between both turbulence models.

As the fluid flow is incompressible, it was used a pressure-based solver with the SIMPLE segregated algorithm (Patankar and Spalding 1972), where the pressure is corrected by enforcing mass continuity over each cell. For the spatial discretization, the convective terms were set by a second order upwind and the pressure with a second-order central-difference scheme. The turbulent variables were solved with a first-order upwind scheme.

RESULTS AND ANALYSIS

In this section the drag generated by each configuration is calculated, also different contours and vectors of the fluid flow around the vehicles are analyzed. Additionally, a brief analysis of the fuel consumption is presented in order to estimate the real advantages of implementing this technology.

AERODYNAMIC ANALYSIS

The drag coefficient of each car carrier configuration is shown in Table 4, where the percentage reduction with respect to the baseline configuration is reported. It is noted that all configurations have less drag than C0; however, C1 and C3 report the greatest drag coefficient reductions, 9.24% and 23.94%, respectively. It is also shown that C3 has the second greatest viscous drag due to the air friction on the surface of the full cover. But, it also has the lowest pressure drag due to the non-interaction between the air and cars transported. On the other hand, C2 has a low drag reduction because it only prevents recirculation of flow entering the sides of the trailer; however, it is noted that the main drag source is the car carrier over the tractor roof. In a study where the crosswind effect was evaluated, this configuration would have more important results.

Table 4. Drag coefficient reduction.

Configurations	Drag Coefficient			
	Viscous	Pressure	Total	diff. [%]
C0	0.020	0.461	0.481	-
C1	0.014	0.422	0.436	9.24
C2	0.009	0.448	0.457	4.96
C3	0.018	0.348	0.366	23.94
C4	0.016	0.446	0.462	3.89
C5	0.011	0.44	0.451	6.18

Numerical results were also analyzed by velocity vectors and contours of pressure and turbulent kinetic energy. The pressure contours and velocity vectors were taken in the symmetry plane of the domain while the turbulent kinetic energy was taken in fourth planes located along the domain separated 6 m between them. In this subsection, only the most relevant results are discussed. In this order, in the first group of simulations ranging from C0 to C3, only C0, C1 and C3 are analyzed.

As discussed above in Table 4, C3 has the greatest drag reduction, which is consistent with Fig. 7, where it shows the lowest flow perturbation and turbulent kinetic energy around and behind the trailer relative to C0 and C1.

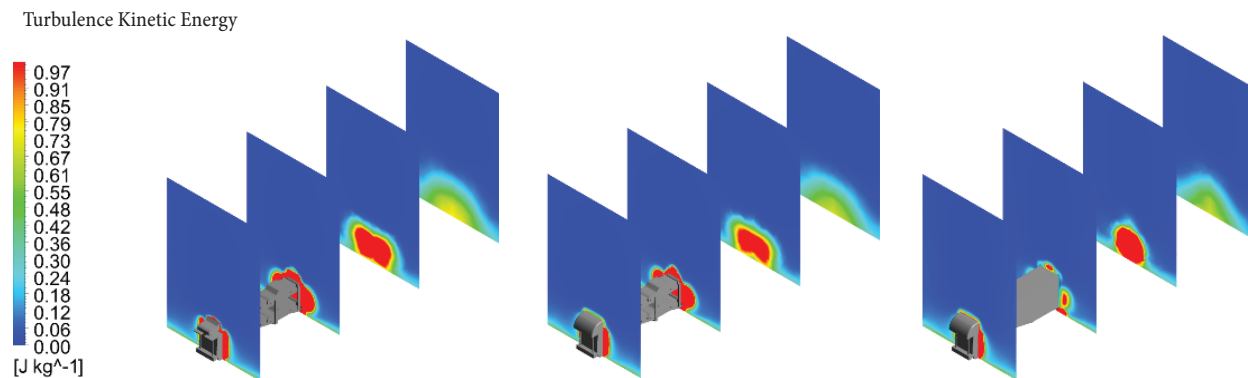


Figure 7. Turbulent kinetic energy contours of (a) C0, (b) C1, and (c) C3.

On the other hand, C1 is a configuration of especial interest since its implementation and operation costs may be lower than C3 although it reduces drag by less than half of C3. C1 has lower turbulence levels than C0, especially on the second floor of the truck and downstream of the trailer, the cover decreases turbulent flow created around the cars transported.

A deeper analysis of C0 and C1 allows us to know the advantage of the latter over the former and to identify the main drag sources in order to improve C1 and achieve on it a greater drag reduction. Figure 8 compares the pressure contours and velocity vectors of C0 and C1. Figures 8a and 8b show that the baseline configuration C0 has high pressure gradients and flow acceleration above the roof of the cars transported on the second floor of the truck. It is also noted that the air can move freely through the gap located above the roof of the tractor cab and generates a recirculation and a low pressure zone behind it increasing the drag. In addition, C1 was proposed to reduce the pressure drag of the truck front and to have a more uniform flow throughout the trailer. Figures 8c and 8d show that the pressure of the front face of the truck is greater than C0, but the pressure gradients are reduced in the second floor and the low pressure behind the tractor increases, which is beneficial for the drag force.

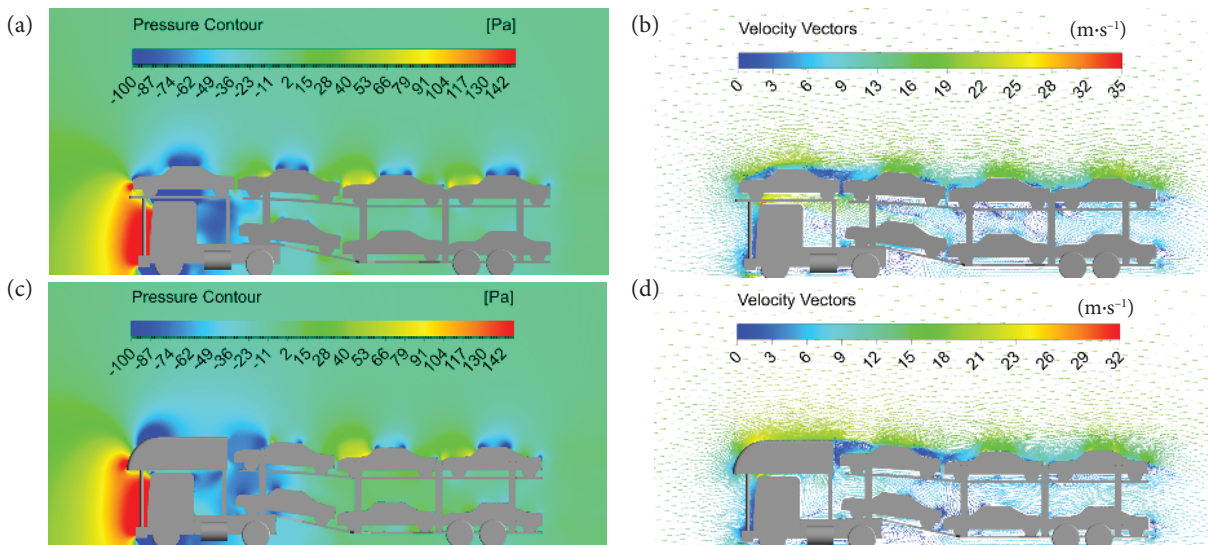


Figure 8. Pressure contours of (a) C0 and (c) C1, and velocity vectors of (b) C0 and (d) C1.

Based on C1, it was proposed configurations C4 and C5; as both configurations present similar pressure contours and velocity vectors, only the C5 results are shown (Fig. 9). C4 and C5 have covers with deflectors located above the cab roof of the truck that detaches the fluid flow reducing the interaction of the air with the trailer, especially on the second floor. However, as is shown in Table 4, results were below the expected due to their drag reductions were lower than C0. As is shown in Figs. 9a and 9b, these

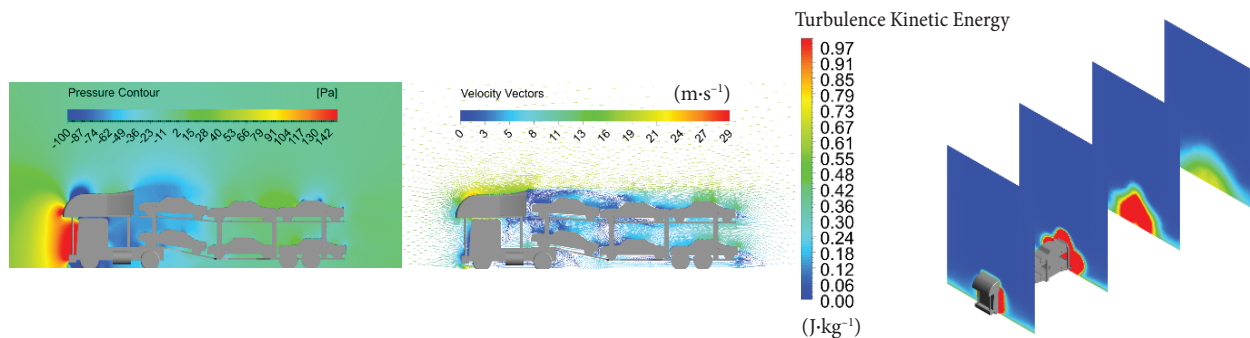


Figure 9. (a) Pressure contours, (b) velocity vectors, and (c) turbulence kinetic energy of C5.

configurations decrease the pressure gradients in the second floor of the trailer and reduce the velocity magnitude through the trailer in relation to C0 and C1; however, the drag of C5 is greater than C1 because the former has a bigger transversal area and a lower mean pressure behind the tractor, therefore the pressure drag is increased. The turbulence kinetic energy of C5, shown in Fig. 9c, is greater than C0 and C1 because the cover side deflection directs the flow away from the truck, increasing the fluid flow perturbation.

FUEL CONSUMPTION ANALYSIS

An analysis of the fuel consumption of the truck was carried out taking into account the additional weight of the covers, but without considering the lift force due to its magnitude is less than 0.1% of the weight of the truck. The total weight for each configuration was calculated assuming covers made of fiberglass and structural steel, which are common materials used in this type of designs. However, a detailed material analysis is beyond the scope of this research.

First, the total force generated by each of the car carrier configurations was calculated at a constant speed of 60 km/h on a straight road. Only aerodynamic and rolling forces were included and the acceleration was neglected. The aerodynamic forces were already calculated in the previous section, and the rolling resistance is calculated based on the total weight of each configuration. The fuel consumption was calculated at sea level under standard conditions, based on Mohamed-Kassim and Filippone (2010). The summary of the results is shown in Table 5. It is noted that the configuration C3, although being the heaviest, has the largest reduction in fuel consumption. Configuration C1 that is one of the lightest, achieves to reduce approximately 50% of the total reduction of C3. Financial analysis should be carried out in order to select what configuration presents greater advantages in real applications.

Table 5. Fuel consumption at 60 km/h.

Configuration	Total weight (Kg)	Rolling resistance force (N)	Drag force (N)	Fuel consumption (l/h)	Fuel saving (%)
C0	35000	1715.00	1088.47	30.92	-
C1	35330	1731.17	986.64	29.97	3.06
C2	35760	1752.24	1034.16	30.73	0.61
C3	36390	1783.11	828.24	28.80	6.85
C4	35330	1731.17	1045.48	30.62	0.95
C5	35330	1731.17	1020.60	30.35	1.84

SUMMARY AND CONCLUSIONS

The fuel consumption due to aerodynamic drag is an important matter for the road transport industry and represents a high economic cost. The car carrier companies are some of the most affected by this issue because the non-aerodynamic shape of their vehicles makes the drag still bigger than a standard semi-trailer truck. In this paper, the CFD analysis of a car carrier with different cover configurations was presented in order to calculate and reduce the aerodynamic drag of the original configuration. The results showed that all proposals reduced the drag of the baseline configuration from 3.9% to 23.9%. The configurations C1 and C3 had the most significant reductions, which reported drag force reductions of 102 N and 260 N, respectively.

The configuration C3 is a classical configuration found in the industry for the drag reduction in heavy trucks with trailer. However, this configuration can represent a high-cost implementation and reduce the versatility for loading and unloading cars relative to the baseline car carrier. Therefore, configuration C1 is an option that could be cheaper than C3 and could keep the loading advantage of the original configuration. Thus, this configuration could be analyzed deeper to improve the drag reduction.

It is important to highlight that heavy trucks are frequently exposed to crosswind during operation, by which the driving stability could be important and the performance of a drag-reduction device could be affected. In future works it will be necessary to analyze these operation conditions to have a detailed performance of the truck with the different covers. Finally, it is required

a deeper economic analysis in order to include variable neglected in this study, like the manufacturing and implementation cost of the configurations, as well as a detailed fuel consumption for a car carrier in long-haul routes.

AUTHOR'S CONTRIBUTION

Conceptualization, Giraldo DA and Palacio DM; Methodology, Navarro JGG; Validation, Botero L and Giraldo DA; Formal analysis, Giraldo DA, Botero L and Navarro JGG; Writing – original draft, Giraldo DA, Palacio DM and Botero L; Writing – review and editing, Giraldo DA, Botero L and Navarro JGG; Visualization, Giraldo DA, Botero L and Navarro JGG; Supervision, Navarro JGG.

REFERENCES

ANSYS (2009) ANSYS Fluent 12.0 User's Guide. ANSYS Inc.

Choi H, Lee J, Park H (2013) Aerodynamics of Heavy Vehicles. *Annual Review of Fluid Mechanics* 46:441-468. doi: 10.1146/annurev-fluid-011212-140616

Chowdhury H, Moria H, Ali A, Khan I, Alam F, Watkins S (2013) A study on aerodynamic drag of a semi-trailer truck. *Procedia Engineering* 56:201-205. doi: 10.1016/j.proeng.2013.03.108

Cooper KR (2003) Truck Aerodynamics Reborn - Lessons from the Past. (2003-01-3376). SAE Technical Paper. doi: 10.4271/2003-01-3376

Davis SC, Williams SE, Boundy RG (2016) Transportation energy data book: edition 35. Oak Ridge: Center for Transportation Analysis Energy and Transportation Science Division.

FHWA (2004) Federal size regulations for commercial motor vehicles. Washington: US Federal Department of Transportation.

Holmberg K, Andersson P, Nylund NO, Mäkelä K, Erdemir A (2014) Global energy consumption due to friction in trucks and buses. *Tribology International* 78:94-114. doi: 10.1016/j.triboint.2014.05.004

Hwang G, Lee S, Lee EJ, Kim JJ, Kim M, You D, Lee SJ (2016) Reduction of drag in heavy vehicles with two different types of advanced side skirts. *Journal of Wind Engineering and Industrial Aerodynamics* 155:36-46. doi: 10.1016/j.jweia.2016.04.009

Hyams DG, Sreenivas K, Pankajakshan R, Nichols DS, Briley WR, Whitfield DL (2011) Computational simulation of model and full scale Class 8 trucks with drag reduction devices. *Computers & Fluids*, 41(1):27-40. doi: 10.1016/j.compfluid.2010.09.015

McCallen RC, Salari K, Ortega JM, Castellucci P, Browand F, Hammache M, Hsu T-Y, Ross J, Satran D, Heineck JT, et al. (2004) DOE's effort to reduce truck aerodynamic drag – joint experiments and computations lead to smart design. Presented at: 34th AIAA Fluid Dynamics Conference and Exhibit; Portland, USA. doi: 10.2514/6.2004-2249

Menter FR (1994) Two-equation eddy-viscosity turbulence models for engineering applications. *AIAA Journal* 32(8):1598-1605. doi: 10.2514/3.12149

Mohamed MH, Ali AM, Hafiz AA (2015) CFD analysis for H-rotor Darrieus turbine as a low speed wind energy converter. *Engineering Science and Technology, an International Journal* 8(1):1-13. doi: 10.1016/j.jestch.2014.08.002

Mohamed-Kassim Z, Filippone A (2010) Fuel savings on a heavy vehicle via aerodynamic drag reduction. *Transportation Research Part D: Transport and Environment* 15(5):275-284. doi: 10.1016/j.trd.2010.02.010

Mosaddeghi F, Oveisi M (2015) Aerodynamic drag reduction of heavy vehicles using append devices by CFD analysis. *Journal of Central South University* 22(12):4645-4652. doi: 10.1007/s11771-015-3015-7

NTG (2007) Permit guidelines for oversize and overmass vehicles. Darwin: Northern Territory Government.

Ortega J, Salari K, Brown A, Schoon R (2007) Aerodynamic drag reduction of class 8 heavy vehicles: a full-scale wind tunnel study. (TR-628153). LLNL Report.

Patankar SV, Spalding DB (1972) A calculation procedure for heat, mass and momentum transfer in three-dimensional parabolic flows. *International Journal of Heat and Mass Transfer* 15(10):1787-1806. doi: 10.1016/0017-9310(72)90054-3

Pabon CAP, Rodriguez AM, Serrano MLE, Yañez MLM, Sagra CT, Morales LS, Perez GG, Maldonado LAR (2011) Diagnostico del transporte. Bogotá: Ministerio de Transporte.

Roy S, Srinivasan P (2000) External flow analysis of a truck for drag reduction. SAE transactions 109:808-812.

Schoon RE (2007) On-road evaluation of devices to reduce heavy truck aerodynamic drag. (2007-01-4294). SAE Technical Paper. doi: 10.4271/2007-01-4294

Shih T-H, Liou WW, Shabbir A, Yang Z, Zhu J (1995) A new $\kappa\text{-}\epsilon$ eddy viscosity model for high reynolds number turbulent flows. Computers & Fluids 24(3):227-238. doi: 10.1016/0045-7930(94)00032-T

Versteeg HK, Malalasekera W (2007) An introduction to computational fluid dynamics: the finite volume method. 2. ed. Glasgow: Pearson Education Limited.

Wickern G, Zwicker K, Pfadenhauer M (1997) Rotating wheels - their impact on wind tunnel test techniques and on vehicle drag results. (970133). SAE Technical Paper. doi: 10.4271/970133

Wood RM (2004) Impact of Advanced Aerodynamic Technology on Transportation Energy Consumption. (2004-01-1306). SAE Technical Paper. doi: 10.4271/2004-01-1306

Wood RM, Bauer SXS (2003) Simple and low-cost aerodynamic drag reduction devices for tractor-trailer trucks. (2003-01-3377). SAE Technical Paper. doi: 10.4271/2003-01-3377